Annals of Nuclear Cardiology Vol. 11 No. 1 20–25

ORIGINAL ARTICLE

Visual Differentiation Between Triglyceride Deposit Cardiomyovasculopathy and Old Myocardial Infarction Using Count-Washout Rate Polar Map in Iodine-123-β-Methyl-p-Iodophenyl-Pentadecanoic Acid Scintigraphy

Ryohei Ono, MD, PhD[1)*], Keisuke Hoshi, MD[2)*], Hideyuki Miyauchi, MD, PhD[1)*] and Yoshio Kobayashi, MD, PhD[1)]

Received: November 5, 2024 / Revised manuscript received: December 23, 2024 / Accepted: January 24, 2025
J-STAGE advance published: September 9, 2025

Abstract

***Background*: In nuclear cardiology, tracer uptake and washout rate (WR) are key parameters for evaluating cardiac pathophysiology. However, WR is influenced by counts in the early image, making it difficult to evaluate pathophysiology based on WR value alone. To differentiate cardiovascular diseases involving count and WR variations, such as triglyceride deposit cardiomyovasculopathy (TGCV) and old myocardial infarction (OMI), we proposed a method to simultaneously evaluate both.**

***Methods*: We newly developed the Count-Washout Rate Polar Map (CWRM), a graphical representation of the count and WR values in a polar coordinate system. CWRM consists of two axes: count in the early image and WR. Given the variety of diseases characterized by count and WR, Iodine-123-β-methyl-p-iodophenyl-pentadecanoic acid was selected as the radiotracer. We examined patients without cardiovascular disease (normal) and patients with TGCV, OMI, and TGCV with OMI. CWRMs for each disease were visually evaluated.**

***Results*: In the normal case, sufficient counts were observed in the early image, and WR did not decrease; CWRM showed light blue. In TGCV, sufficient counts were observed in the early image, but WR markedly decreased; CWRM showed orange evenly. In non-TGCV with OMI, regions with decreased and preserved counts coexisted; CWRM showed light blue in the normal region and black in the OMI region. In TGCV with OMI, CWRM showed orange in the TGCV myocardium and black in the OMI region.**

***Conclusion*: CWRM is useful for at-a-glance differentiation of patients with TGCV, OMI, and TGCV with OMI, thereby showing potential as a new diagnostic indicator.**

Keywords: Count-washout rate polar map, Iodine-123-β-methyl-p-iodophenyl-pentadecanoic acid (^{123}I-BMIPP), Myocardial infarction, Single-photon emission computed tomography (SPECT), Triglyceride deposit cardiomyovasculopathy (TGCV), Washout rate

Ann Nucl Cardiol 2025; 11 (1): 20–25

In nuclear medicine, tracer uptake and washout rate (WR) are utilized to differentiate various diseases. Combining these two indicators could facilitate a comprehensive understanding of pathological conditions and potentially enhance disease diagnoses (1, 2). However, several factors can influence these indicators, necessitating the consideration of their interrelationship when evaluating pathological conditions. Specifically, a decrease in uptake in the early image affects WR. In other words, uptake and WR are not entirely independent indicators.

DOI: 10.17996/anc.24-00012

1) Department of Cardiovascular Medicine, Chiba University Graduate School of Medicine, Chiba, Japan
2) Department of Pediatrics, Ohta General Hospital Foundation Ohta Nishinouchi Hospital, Fukushima, Japan

*These authors equally contributed to this work.

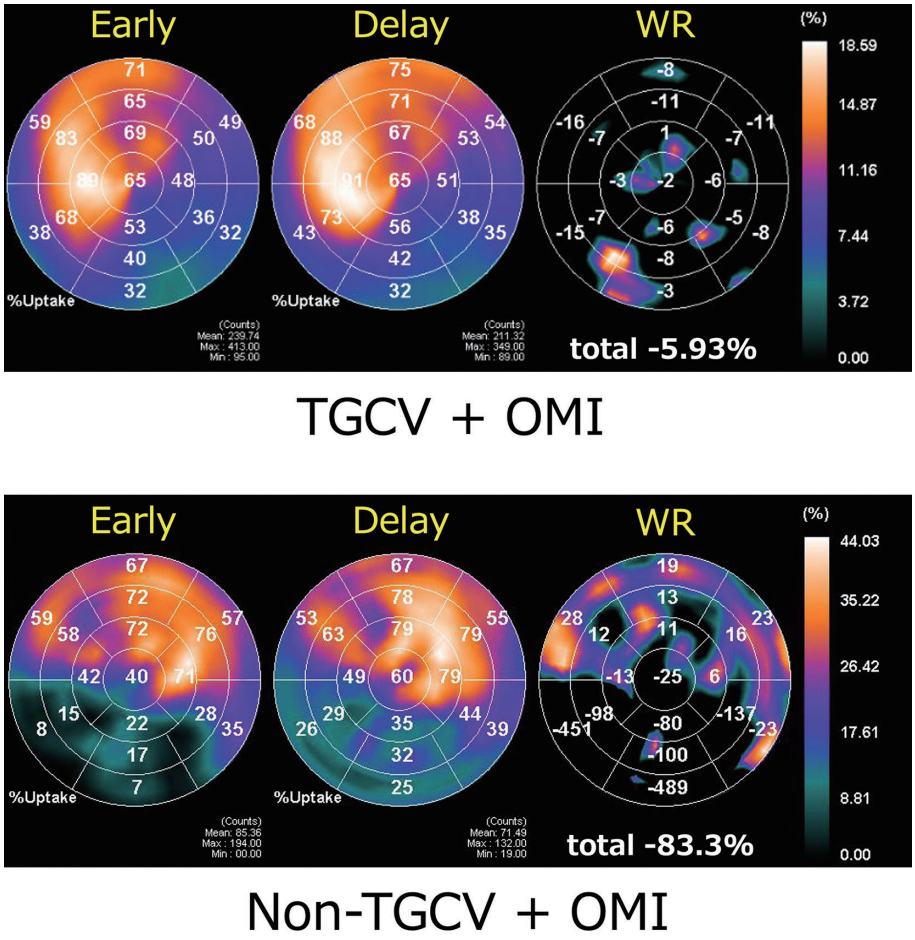

Figure 1 ^{123}I-BMIPP SPECT polar maps of TGCV and non-TGCV with OMI. As illustrated, the WR value of TGCV with OMI is -5.93%, whereas that of non-TGCV with OMI is -83.3%.
OMI, old myocardial infarction; TGCV, triglyceride deposit cardiomyovasculopathy; WR, washout rate.

WR is calculated using either planar imaging data or single-photon emission computed tomography (SPECT) data. For SPECT, segments from the polar map (which represents the entire left ventricle) that correspond to the region of interest (either the entire left ventricle or a part of it) are extracted, and the average WR of these segments is used. WR is defined as the ratio of the difference between the count in the early image and the time-decay-corrected delayed image divided by the former (2–4). Based on this calculation method, low counts in early images will result in a low WR. For instance, old myocardial infarction (OMI) can cause defective regions of perfusion tracers (^{201}Tl and ^{99m}Tc-tetrofosmin) uptake and fatty acid metabolism tracer (Iodine-123-β-methyl-p-iodophenyl-pentadecanoic acid; ^{123}I-BMIPP) uptake in both early and delayed images, leading to a markedly decreased WR for such lesions.

Conversely, one condition in cardiomyocytes characterized by a decrease in ^{123}I-BMIPP WR is known as triglyceride deposit cardiomyovasculopathy (TGCV), which involves defective intracellular lipolysis and triglyceride accumulation at the cellular level (5, 6). Although the cardiomyocytes of patients with TGCV show a decreased ^{123}I-BMIPP WR, fatty acids are properly taken up, thereby preserving the ^{123}I-BMIPP uptake in the early images.

Practice recommendation for measuring WR in ^{123}I-BMIPP images noted that when patients have large metabolic defects due to OMI or severe fibrosis, defective segments can decrease regional WRs (3, 4). For instance, decreased ^{123}I-BMIPP uptake in the early images, seen in OMI, would cause a markedly decreased WR, and it is difficult to distinguish between TGCV with OMI and non-TGCV with OMI based on low WR values alone (Figure 1). Therefore, focusing only on the low WR makes it difficult to differentiate pathologies, and it is necessary to simultaneously evaluate both uptake in the early image and WR. To differentiate cardiovascular diseases that involve tracer uptake and WR variations, such as TGCV and OMI, we developed a novel technique called the Count-Washout Rate Polar Map (CWRM).

Materials and methods

Selection of participants and radiotracer

We examined patients without cardiovascular disease

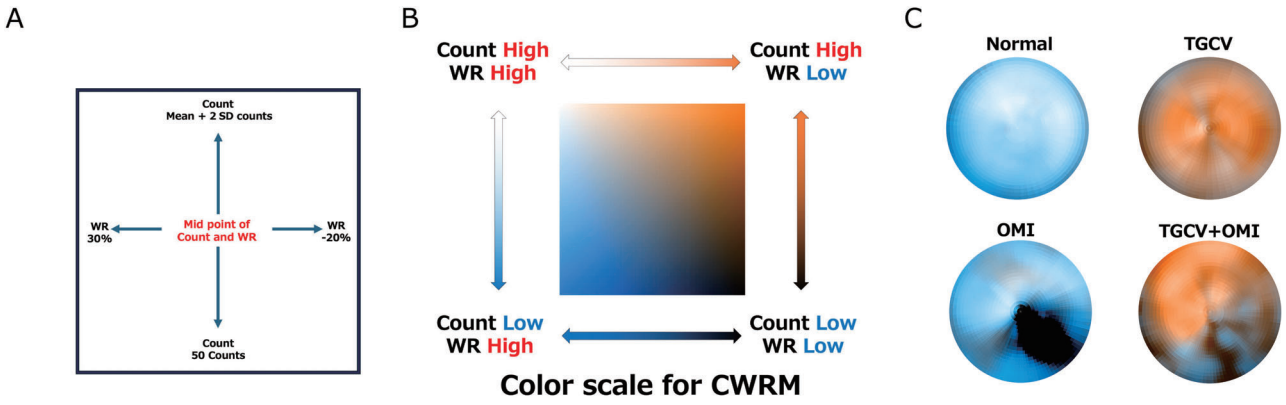

Figure 2　Count-washout rate polar map (CWRM).
A: Allocation of counts and WR in orthogonal coordinates for CWRM: the vertical axis represents count; and the horizontal axis, WR. The count window is set to a maximum of the mean + 2 SD and a minimum of 50 counts, while the WR window is set to a maximum of 30% and a minimum of -20%. The center of the scale is the midpoint of each range.
B: Color scale for CWRM. The color scale is set as follows. High count and high WR are represented by white. Low count and high WR are represented by blue. High count and low WR are represented by orange. Low count and low WR are represented by black.
C: Visualization of each disease using CWRM: CWRMs show light blue in the normal case and orange in the case of TGCV. In non-TGCV with OMI, CWRM shows light blue in the normal region and black in the OMI region. In TGCV with OMI, CWRM shows orange in the TGCV myocardium and black in the OMI region.
OMI, old myocardial infarction; SD, standard deviation; TGCV, triglyceride deposit cardiomyovasculopathy; WR, washout rate.

(normal) and patients with TGCV, OMI, or TGCV with OMI, as these conditions exhibit variations in uptake and WR. TGCV is characterized by decreased ^{123}I-BMIPP WR due to impaired intracellular fatty acid metabolism, while OMI regions exhibit low ^{123}I-BMIPP WR due to myocardial necrosis. Given the various pathologies causing decreased uptake and WR, ^{123}I-BMIPP was selected as the radiotracer for this study. Although several cases for each disease were examined to validate the concept of CWRM in this study, representative cases were presented in the results. This study was approved by the Research Ethics Committee of Chiba University Graduate School of Medicine (#4159).

Study protocol

Following the protocol recommended by the Japanese Society of Nuclear Cardiology, after fasting for ≥12 hours, 111 MBq of ^{123}I-BMIPP (Cardiodine; Nihon Medi-Physics Co. Ltd., Tokyo, Japan) was intravenously injected at rest. Early and delayed images were obtained after 20 and 210 minutes, respectively. The SPECT system used was NM/CT 870 DR (GE Healthcare Japan, Tokyo, Japan), equipped with an extended low-energy general-purpose collimator. The collection was performed in a 64 × 64 matrix in 180° step and shoot mode in a circular orbit with a 6° sampling angle and 60 seconds/view. The pixel size and slice width were both 5.89 mm. The energy windows for ^{123}I were 159 keV ± 10%. Reconstruction was performed with scatter corrections using filtered back-projection (using a ramp filter) and a 10th-order Butterworth filter with 0.4 cycle/cm cutoff frequency.

SPECT analysis software

SPECT data analysis for WR calculation used Heart Risk View-S (Nihon Medi-Physics, Co. Ltd., Tokyo, Japan). This dedicated software analyzes myocardial perfusion semi-automatically, provides polar maps, and calculates the WR. Heart Risk View-S can export a Comma-Separated Values (CSV) file containing the data of counts and WRs for each of 2,400 segments (20 rows and 120 columns) of the left ventricle (LV) (2).

Count-washout rate polar map (CWRM)

We created a two-dimensional color scale, with the vertical axis representing the count and the horizontal axis representing the WR (Figure 2A). To create CWRM, the maximum and minimum values for the axis windows of count and WR for each case were first determined. The count window was set to a maximum of the mean plus two standard deviations (SD) and a minimum of 50 counts, while the WR window was set to a maximum of 30% and a minimum of -20%. The midpoint of each range was set as the center of the heat map. The color scale was uniquely determined using orthogonal coordinates.

For the color scale, we used the following scheme and created CWRM (Figure 2B).

- High count and high WR are represented by white.
- Low count and high WR are represented by blue.
- High count and low WR are represented by orange.

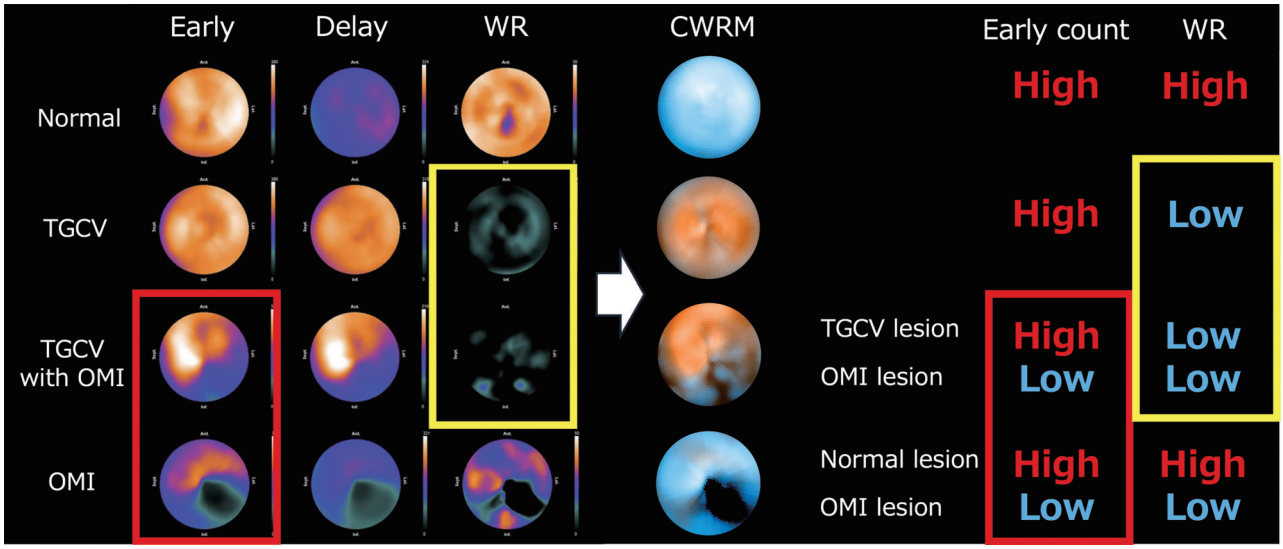

Figure 3 ^{123}I-BMIPP SPECT polar maps of the early, time-decay-corrected delayed, and WR images and CWRM for each disease.

The areas highlighted in red (early images) and yellow (WR images) respectively show similar polar maps but different diseases.

CWRM, count-washout rate map; OMI, old myocardial infarction; TGCV, triglyceride deposit cardiomyovasculopathy; WR, washout rate.

・Low count and low WR are represented by black.

The color combinations of blue and orange, as well as white and black, were selected for their strong visual contrasts. Using this color scale, we can easily identify and interpret the varying degrees of tracer uptake and WR in the polar map. For each segment data exported from the CSV file of Heart Risk View-S, the early image counts and WR values were applied to the color scale and displayed in the polar coordinate system of CWRM.

Detailed process of CWRM creation

CSV file data containing 2,400 segments (20 rows and 120 columns) of counts in the early image and WR were retrieved from each participant. For example, in the normal case, the maximum and minimum early counts in the 2,400 segments were 303.39 and 116.22 counts, respectively. In addition, the mean and SD were calculated as 241.49 and 38.52 counts, respectively. Therefore, the upper count window was set at 318.53, calculated as the mean + 2 SD. On the other hand, the maximum and minimum WRs in the 2,400 segments were 44.44 % and 17.06 %, respectively. Next, color gradation was set according to the following rules: the maximum windows of both the count in the early image and the WR is in white; the maximum window of the WR and minimum window of the count in the early image is in blue; the maximum window of the count in the early image and minimum window of the WR is in orange; and the minimum windows of both the count in the early image and the WR is in black. For each segment, the early image counts and WR values were applied to this color gradation scale and displayed two-dimensionally in the polar coordinate system of CWRM.

Results

CWRMs of each disease

CWRMs of each disease are shown in Figure 2C. In the normal case, sufficient counts were observed in the early images, and the WR did not decrease; CWRM displayed light blue. In TGCV, sufficient counts were observed in the early images, but the WR markedly decreased; CWRM displayed an even distribution of orange. In non-TGCV with OMI, the regions with decreased and preserved counts coexisted; CWRM showed light blue in the normal region and black in the OMI region. In TGCV with OMI, CWRM showed orange in the TGCV myocardium and black in the OMI region. As a result, the OMI region was represented in black regardless of whether the myocardium was TGCV or not. However, normal myocardium and TGCV myocardium could be differentiated due to their distinct colors, light blue and orange, respectively, thereby allowing for a clear separation between these two pathological conditions.

^{123}I-BMIPP SPECT polar map displays and CWRM

Figure 3 shows the conventional ^{123}I-BMIPP SPECT polar map displays (early images, time-decay-corrected delayed images, and WR maps) and CWRM for each disease. In the normal case, the early count is sufficient throughout the LV, and WR is preserved in all areas. In the TGCV case, the early tracer uptake is entirely sufficient in the LV, but WR decreases throughout. In the case of TGCV with OMI, high tracer uptake in the TGCV regions and low tracer uptake in the OMI regions

coexist in the early image, but WR is entirely decreased. Finally, in the case of OMI, high uptake in the normal regions and low uptake in the OMI regions coexist in the early image, and WR is preserved in the normal regions and decreased in the OMI regions.

Discussion

In this study, we developed a novel technique called CWRM, a graphical representation of tracer uptake and WR values in a polar coordinate system. CWRM successfully achieved the visual differentiation of patients with TGCV, OMI, and TGCV with OMI.

Since tracer uptake and WR have conventionally been displayed on separate polar maps, physicians have combined both parameters cognitively to interpret the pathology; however, this approach lacks objectivity and makes shared interpretation difficult. Combining these two indicators would enhance the precision of disease identification and classification, improving the accuracy of diagnostic processes. Therefore, we investigated whether these parameters, which have conventionally been considered separate, can be conceptually integrated into a single entity using CWRM. The advantage of this study is its ability to simultaneously represent both tracer uptake and WR values on a single polar map, allowing for visual differentiation of pathological conditions.

When focusing solely on the early image or WR in Figure 3, it is challenging to distinguish the areas highlighted in red and yellow respectively because these polar maps appear quite similar. To address this problem, we developed a novel technique of CWRM and successfully achieved visual differentiation for TGCV, OMI, and TGCV with OMI. To the best of our knowledge, this is the first attempt to represent count and WR simultaneously using a polar coordinate system. CWRM provides a novel approach for understanding two parameters simultaneously and distinguishing diseases visually.

For future perspectives, visual classification using CWRM can be applied to other cardiovascular diseases with counts and WR variations. Although we currently use a 2 x 2 color combination, in the future, we may need to change the range setting or consider different color combinations for more detailed counting and WR differentiation. Also, CWRM could potentially be useful in tracking pathological changes over time. Furthermore, we consider that the concept of CWRM can be extended to other nuclear imaging tracers, as many nuclear cardiology images feature two parameters. For example, stress/rest myocardial perfusion imaging can potentially examine the rest-stress difference in a single image; another possible application is iodine-123 meta-iodobenzylguanidine scintigraphy for assessing myocardial sympathetic nerve activity or prognosis by integrating its uptake and washout in a single image.

Study limitations

The present study has several limitations. As a pilot study, the validation for other cardiovascular diseases is limited. The CWRM is a qualitative rather than a quantitative data analysis approach, and its interpretation may be influenced by the subjectivity of the physicians. Additionally, the CWRM relies on visual classification, but observers may perceive colors differently. Each institution has different imaging and collection conditions for ^{123}I-BMIPP SPECT, resulting in non-standardized color scale settings for CWRM, which can vary between institutions.

Conclusions

In conclusion, CWRM is effective for visually differentiating patients with TGCV, OMI, and TGCV with OMI. CWRM provides a novel approach for understanding the two parameters of counts and WR simultaneously and distinguishing diseases visually.

Acknowledgments

None.

Author contribution

RO and HM wrote the main manuscript. HM proposed the concept of this manuscript. KH designed the software to realize the concept, and implemented it after thorough discussions with HM.

Data analyses were conducted by HM, and verified by RO, KH, and HM. YK provided comments throughout the entire content.

Sources of funding

None.

Conflicts of interest

None.

Reprint requests and correspondence:
Hideyuki Miyauchi, MD, PhD
Department of Cardiovascular Medicine, Chiba University Graduate School of Medicine, 1-8-1 Inohana, Chuo-ku, Chiba 260-8670, Japan
E-mail: hmiyauchi@chiba-u.jp

References

1. Giedd KN, Bergmann SR. Fatty acid imaging of the heart. Curr Cardiol Rep 2011; 13: 121–31.
2. Miyauchi H, Ono R, Iimori T, et al. Modified algorithm using total count for calculating myocardial washout rate in single-photon emission computerized tomography. Ann Nucl Cardiol 2023; 9: 19–25.
3. Nakajima K, Miyauchi H, Hirano KI, et al. Practice recommendation for measuring washout rates in ^{123}I-BMIPP fatty acid images. Ann Nucl Med 2024; 38: 1–8.
4. Nakajima K, Miyauchi H, Hirano KI, et al. Practice recommendation for measuring washout rates in ^{123}I-BMIPP fatty acid images. Ann Nucl Cardiol 2023; 9: 3–10.
5. Hirano K, Ikeda Y, Zaima N, Sakata Y, Matsumiya G. Triglyceride deposit cardiomyovasculopathy. N Engl J Med 2008; 359: 2396–8.
6. Kobayashi K, Sakata Y, Miyauchi H, et al. The diagnostic criteria 2020 for triglyceride deposit cardiomyovasculopathy. Ann Nucl Cardiol 2020; 6: 99–104.